A&A 553, A42 (2013)
DOI: 10.1051/0004-6361/201220957

Astronomy & Astrophysics

Radiative association of He_2^+ revisited

L. Augustovičová[1], V. Špirko[2], W. P. Kraemer[3], and P. Soldán[4,⋆]

[1] Charles University in Prague, Faculty of Mathematics and Physics, Department of Chemical Physics and Optics, Ke Karlovu 3, 12116 Prague 2, Czech Republic
e-mail: lucie.augustovicova@mff.cuni.cz
[2] Institute of Organic Chemistry and Biochemistry, Academy of Sciences of the Czech Republic, Flemingovo nám. 2, 16010 Prague 6, Czech Republic
e-mail: vladimir.spirko@marge.uochb.cas.cz
[3] Max-Planck-Institute of Astrophysics, Postfach 1371, 85741 Garching, Germany
e-mail: wpk@mpa-garching.mpg.de
[4] Charles University in Prague, Faculty of Mathematics and Physics, Department of Chemical Physics and Optics, Ke Karlovu 3, 12116 Prague 2, Czech Republic
e-mail: pavel.soldan@mff.cuni.cz

Received 19 December 2012 / Accepted 13 March 2013

ABSTRACT

Aims. Rate coefficients for spontaneous and stimulated radiative association of the He_2^+ molecular ion are presented as a function of temperature, considering the association with rotational-vibrational states of the ground X electronic state from the continuum states of the lowest three excited A, C, and E electronic states.
Methods. The rate coefficients are obtained from the cross sections for radiative association, which are calculated by solving the Schrödinger equation for bound and continuum states supported by the corresponding Born-Oppenheimer potential energy curves.
Results. The rate coefficients for the $A \rightarrow X$ spontaneous process are in excellent agreement with previous calculations. For temperatures up to about 10 000 K, the spontaneous $C \rightarrow X$ and $E \rightarrow X$ processes are dominant, exceeding the $A \rightarrow X$ rate coefficient by several orders of magnitude. Stimulation of the radiative association by black-body radiation has significant influence only on the $A \rightarrow X$ process at temperatures below 1000 K. The black-body radiation temperature would have to be well above 50 000 K in order to have any noticeable effect on the $C \rightarrow X$ and $E \rightarrow X$ processes.

Key words. molecular processes

1. Introduction

The small diatomic ions H_2^+ or HeH^+ and He_2^+ are assumed to be significantly abundant in the atmospheres of white dwarf stars, either in the hydrogen-dominated DA-type stars or the less numerous helium-rich ones, respectively (Koester & Chanmugam 1990). Continuous absorption by these ions has been shown to be a major source of the opacity in the ultraviolet continuum of these stars (Stancil 1994). With their one-dimensional potentials originating from solutions of a small few-electron problem, these ions can be treated on very high theoretical accuracy levels and are therefore ideal test cases for comparisons between theory and results obtained from laboratory experiments or observations.

There have been numerous accurate theoretical studies of the $X^2\Sigma_u^+$ ground electronic state of the He_2^+ ion, culminating in the highly accurate calculations of its adiabatic potential energy curve by Cencek & Rychlewski (1995) and most recently in calculations of the ground state potential including adiabatic corrections by Tung et al. (2012). Theoretical studies on a similar high accuracy level of the excited states are less frequent, which is partly due to the fact that within the adiabatic approximation these states undergo numerous avoided curve crossings. The first serious attempt to clear up the situation for the lowest six $^2\Sigma_g^+$ excited states went beyond the adiabatic Born-Oppenheimer approximation, evaluating in addition to the adiabatic potential curves the non-adiabatic matrix elements at the avoided crossings and thus constructing approximate diabatic potential curves (Metropoulos et al. 1987). Other extended calculations focused later on the Born-Oppenheimer potentials of the low-lying $^2\Sigma_u$, $^2\Sigma_g$, $^2\Pi_u$, and $^2\Pi_g$ states (Ackermann & Hogreve 1991; Bawagan & Davidson 1997). Recently, a two-state study of the ground and first excited states was performed, which included an exact treatment of all adiabatic correction terms (Xie et al. 2005).

Stancil et al. (1993) have studied the spontaneous radiative-association formation of He_2^+ from collisions of He^+ ions with He atoms in their ground state and discussed possible astrophysical implications of this reaction in attempts to model abundances in SN 1987A ejecta and in the planetary nebula NGC 7027. They came to the conclusion that the formation of He_2^+ in the early Universe does not have any interesting consequences. In contrast, the helium-containing small molecular ions HeH^+ and He_2^+ are known to be highly abundant in the atmospheres of He-rich white dwarf stars (Gaur et al. 1988, 1992) and some planetary nebulae (Black 1978; Flower & Roueff 1979; Stancil 1994). It was demonstrated, for instance, that HeH^+ can affect significantly the photosphere of such stars (Harris et al. 2004) and that the resulting increased opacity will lengthen their cooling time (Fontaine et al. 2001). The same holds for contributions from $He + He^+$ collisional absorption and He_2^+ photo-dissociation processes (Ignjatovic et al. 2009). Since temperatures in these objects are very high, investigations of possible interactions

⋆ The corresponding author.

between excited He atoms and He^+ ions or protons seem to be appropriate.

On this background the present study intends to go beyond the previous work of Stancil et al. (1993), investigating the different radiative-association formation processes of He_2^+, which can be formulated with the lowest three excited $^2\Sigma_g^+$ states acting as reactant channels. They are described as

$$A^2\left[\mathrm{He}(1^1S) + \mathrm{He}^+\right]_g \rightarrow \mathrm{He}_2^+(X^2\Sigma_u^+) + h\nu \;\; (A \rightarrow X) \quad (1)$$

$$C^2\left[\mathrm{He}(2^3S) + \mathrm{He}^+\right]_g \rightarrow \mathrm{He}_2^+(X^2\Sigma_u^+) + h\nu \;\; (C \rightarrow X) \quad (2)$$

$$E^2\left[\mathrm{He}(2^1S) + \mathrm{He}^+\right]_g \rightarrow \mathrm{He}_2^+(X^2\Sigma_u^+) + h\nu \;\; (E \rightarrow X), \quad (3)$$

where $^2[\ldots]_g$ means a doublet g submanifold of the corresponding collisional continuum. According to this scheme, reactions start from collisions of He in one of the lowest three atomic levels (1^1S, 2^3S, 2^1S) with He^+ ions and proceed via resonance and continuum states of the excited $A^2\Sigma_g^+$, $C^2\Sigma_g^+$, and $E^2\Sigma_g^+$ potentials of the collisional complex to form under spontaneous photon emission the molecular-ion ground state $X^2\Sigma_u^+$. These processes are characterized in the above scheme as $A \rightarrow X$, $C \rightarrow X$, or $E \rightarrow X$, respectively. Apart from spontaneous emission, processes stimulated by the background radiation with frequency ν_b (Stancil & Dalgarno 1997; Zygelman et al. 1998) are also considered:

$$\mathrm{He}^* + \mathrm{He}^+ + h\nu_b \rightarrow \mathrm{He}_2^+ + h\nu + h\nu_b. \quad (4)$$

The underlying information necessary for the present dynamics calculations, i.e. potential energy data for the different He_2^+ states and the dipole transition data, is calculated on a high accuracy level of ab initio theory (details of these calculations and a discussion of the methodology used will be collected in a separate paper (Augustovičová et al., in prep.).

2. Methods

In quantum mechanics, the cross sections for radiative association of a diatomic molecule in the presence of black-body radiation can be expressed as a sum over allowed transitions between a continuum state with a positive energy E and orbital angular momentum N' to bound rovibrational states with vibrational quantum number v'' and orbital angular momentum N'' (Zygelman & Dalgarno 1990):

$$\sigma(E;T_b) = \sum_{N',v'',N''} \sigma_{N';v'',N''}(E;T_b), \quad (5)$$

where the temperature T_b characterizes the black-body radiation field. In the case of dipole moment transitions, the individual cross sections can be expressed as (Stancil & Dalgarno 1997)

$$\sigma_{N';v'',N''}(E;T_b) = \frac{1}{4\pi\epsilon_0}\frac{64}{3}\frac{\pi^5}{c^3\,k^2}\, p\, \nu_{E;v'',N''}^3\, S_{N',N''}\, M_{E,N';v'',N''}^2 \times\left[\frac{1}{1-\exp\left(-h\nu_{E;v'',N''}/k_B T_b\right)}\right], \quad (6)$$

where c is the speed of light in a vacuum, $k^2 = 2\mu E/\hbar^2$, μ is the "reduced mass" of the molecular ion (μ = 3647.89986 AU for $^4He_2^+$), p is the probability of approach in the initial electronic state ($p = 1/2$ for $A \rightarrow X$ and $E \rightarrow X$ and $p = 1/6$ for $C \rightarrow X$), and $\nu_{E;v'',N''}$ is the emitted photon frequency, $h\nu_{E;v'',N''} = E + \Delta E - E_{v'',N''}$, where $\Delta E = 0$ cm^{-1} for $A \rightarrow X$, $\Delta E = 19.8176$ eV for $C \rightarrow X$ and $\Delta E = 20.6164$ eV for $E \rightarrow X$ (Ralchenko et al. 2010).

For a homonuclear diatomic molecule within the Hund's case (a) spin-less approximation, the dipole moment transitions between Σ_g and Σ_u states are governed by the rotational selection rules $\Delta N = N' - N'' = \mp 1$. Thus there are only two branches and the only non-zero Hönl-London coefficients are $S_{N',N'+1} = N'+1$ and $S_{N',N'-1} = N'$, respectively.

$$M_{E,N';v'',N''} = \int_0^\infty \chi_{N'}(E,R)\, d_z(R)\, \psi_{v'',N''}(R)\, \mathrm{d}R \quad (7)$$

is the matrix element of the transition dipole moment function $d_z(R)$ between the initial continuum radial wave function $\chi_{N'}(E,R)$ for the partial wave N' and the final bound-state radial wave function $\psi_{v'',N''}(R)$. The above formula (6) is derived for the energy-normalized continuum wave function $\chi_{N'}(E,R)$:

$$\chi_{N'}(E,R) \sim \left(\frac{2\mu}{\hbar^2\pi k}\right)^{1/2} \sin\left[kR - \frac{1}{2}N'\pi + \delta_{N'}(E)\right] \quad \text{for } R \rightarrow \infty, \quad (8)$$

where $\delta_{N'}(E)$ is the phase shift and

$$\int_0^\infty |\psi_{v'',N''}(R)|^2\, \mathrm{d}R = 1. \quad (9)$$

Moreover, in the case of a homonuclear diatomic molecule with zero nuclear spin (such as $^4He_2^+$), symmetry requires that only even N' levels are populated in the Σ_g electronic states and only odd N'' levels are populated in the Σ_u electronic states. Thus the sum in Eq. (5) goes only over even N', and then the Hönl-London coefficients conveniently arrange that it also goes only over odd N''.

The radial wave functions may be determined by numerical integration of the Schrödinger equations

$$\left[-\frac{\hbar^2}{2\mu}\frac{\mathrm{d}^2}{\mathrm{d}R^2} + \frac{\hbar^2}{2\mu}\frac{N'(N'+1)}{R^2} + U_C(R)\right]\chi_{N'}(E,R) = E\,\chi_{N'}(E,R), \quad (10)$$

$$\left[-\frac{\hbar^2}{2\mu}\frac{\mathrm{d}^2}{\mathrm{d}R^2} + \frac{\hbar^2}{2\mu}\frac{N''(N''+1)}{R^2} + U_B(R)\right]\psi_{v'',N''}(R) = E_{v'',N''}\,\psi_{v'',N''}(R), \quad (11)$$

where $U_C(R)$ and $U_B(R)$ are the potential energy functions supporting the initial continuum state E, N' and the final bound state v'', N'', respectively. The wave functions $\chi_{N'}(E,R)$ and $\psi_{v'',N''}(R)$ were calculated by numerical integration of the radial Schrödinger equation using the Numerov-Cooley method (Numerov 1933; Cooley 1961). Resonance positions and tunneling widths were calculated employing the computer program LEVEL 7.7 (Le Roy 2005) and making use of the Airy-function boundary condition at the outermost classical turning point (Le Roy & Liu 1978) and the uniform semiclassical method (Connor & Smith 1981; Huang & Le Roy 2003).

For evaluation of the continuum and bound-state wave functions in Eqs. (10, 11) and the dipole moment matrix elements in Eq. (7), it is necessary to have either analytical or numerical representation of the potential energy and dipole moment functions. We chose numerical representation by the one-dimensional reciprocal-power reproducing kernel Hilbert space (RP-RKHS) interpolation method (Ho & Rabitz 1996). This

Table 1. Molecular characteristics of the potential energy curves used in the cross-section calculations of the He_2^+ radiative association.

State	R_e (a_0)	$\mathcal{D}_e$ (cm^{-1})	$\mathcal{D}_0$ (cm^{-1})	ΔE (eV)
$X^2\Sigma_u^+$	2.042[a]	19 954.583[a]	19 113.978[a]	0
$A^2\Sigma_g^+$	8.718	17.516	8.185	0
$C^2\Sigma_g^+$	6.837	9 172.316	9024.917	19.8176[b]
$E^2\Sigma_g^+$	15.358	733.800	699.762	20.6164[b]

Notes. R_e is the position of the global minimum (equilibrium distance), $\mathcal{D}_e$ is the dissociation energy from the potential global minimum, $\mathcal{D}_0$ is the dissociation energy from the lowest rovibrational state, ΔE is the energy gap between the corresponding dissociation limits. [(a)] The Born-Oppenheimer potential energy curve from Tung et al. (2012) was used for the $X^2\Sigma_u^+$ state. [(b)] Experimental values from Ralchenko et al. (2010) were used for ΔE.

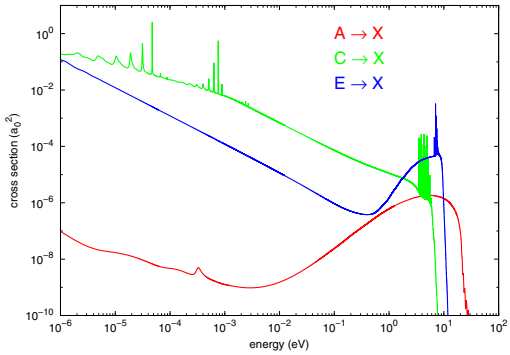

Fig. 1. Cross sections for spontaneous (T_b = 0 K) radiative association of He_2^+. Only the contribution of resonances wider than 0.1 cm^{-1} is shown.

method allows not only for qualitatively correct extrapolation in the long-range region of the $A + A^+$ interaction potential

$$U(R) \sim -\frac{D_4}{R^4} - \frac{D_6}{R^6} \quad \text{for } R \to \infty, \tag{12}$$

but also for the use of predetermined values of long-range coefficients (Ho & Rabitz 2000). In the case of potential energy curves U, the interpolation was done with respect to r^2 (Soldán & Hutson 2000) using RP-RKHS parameters $m = 1$ and $n = 2$, the coefficient D_4, which is equal to $\alpha_d/2$, was kept fixed to the values given by static dipole polarisabilities $\alpha_d[He(1^1S)] = 1.383191$ AU (Pachucki & Sapirstein 2000), $\alpha_d[He(2^3S)] = 800.31633$ AU and $\alpha_d[He(2^1S)] = 315.631468$ AU (Yan & Babb 1998). Very accurate interaction energies of the ground $X^2\Sigma_u^+$ state (Tung et al. 2012) were exploited as known data points for the interpolation. We calculated ab initio interaction energies for the excited states $A^2\Sigma_g^+$, $C^2\Sigma_g^+$, and $E^2\Sigma_g^+$ and the corresponding transition dipole moment values employing the multi-reference configuration interaction method (combined with a very large electron basis set) as implemented in the quantum chemistry program suite MOLPRO (Werner et al. 2010). Further details of these extensive quantum chemistry calculations will be published later elsewhere (Augustovičová et al., in prep.).

Having obtained the corresponding cross sections (5), the rate coefficients for formation of a molecule by (spontaneous and stimulated) radiative association at temperature T is then defined by

$$\alpha(T;T_b) = \left(\frac{8}{\mu\pi}\right)^{1/2}\left(\frac{1}{k_B T}\right)^{3/2}\int_0^\infty E\,\sigma(E;T_b)\,e^{-E/k_B T}\,dE. \tag{13}$$

To evaluate this integral as accurately as possible, we followed the approach of Augustovičová et al. (2012), where contributions from wide and narrow resonances are treated separately from the background contribution. This method was successfully used for very recent calculations of radiative-association rate coefficients of the molecular ion $LiHe^+$ (Augustovičová et al. 2012).

3. Results and discussion

Using the high-level calculations of Tung et al. (2012) for the $X^2\Sigma_u^+$ state as reference, we calculated the potentials of the three lowest $^2\Sigma_g^+$ states on a comparable accuracy level. In Table 1 some data characterizing the three excited states potentials are summarized. For the A state, degenerate with the X state at dissociation, the equilibrium bond distance R_e and the dissociation energy $\mathcal{D}_e$ are in perfect agreement with previous accurate results obtained by Xie et al. (2005) and those of Carrington et al. (1995). Relative to the results of Xie et al. (2005), the present R_e is smaller by less than 0.3 percent and $\mathcal{D}_e$ is larger by less than 1 percent. For the C state, R_e and $\mathcal{D}_e$ can be compared with earlier calculations by Ackermann & Hogreve (1991), which were performed at a lower accuracy level. Whereas the difference in R_e is only about 0.9 percent, $\mathcal{D}_e$ differs considerably more: 9173 cm^{-1} compared to 8565 cm^{-1}. For the E state, accurate results for comparison are not available. Quantitative comparisons with the corresponding basic data used in the white dwarf atmosphere studies of Stancil et al. (1993), Stancil (1994), and Ignjatovic et al. (2009) are not possible, because explicit numerical results are not given there. However, the qualitative agreement with these studies is very good. The $X^2\Sigma_u^+$ potential energy curve of Tung et al. (2012) supports 409 rotational-vibrational bound states as opposed to 411 states found by Stancil et al. (1993). Our maximum rotational quantum numbers differ from those presented by Stancil (1994) for four vibrational states (for $v = 1, 11, 20$, and 23 our N_{max} are 55, 35, 13, and 3, respectively). The $X^2\Sigma_u^+$ potential energy curve of Tung et al. (2012), our $A^2\Sigma_g^+$ potential energy curve, and our transition dipole moment function connecting these two states also seem to agree very well with the corresponding function plots of Ignjatovic et al. (2009) with no visible differences.

Cross sections for a spontaneous (T_b = 0 K) radiative association are shown graphically in Fig. 1. The cross sections for the $C \to X$ and $E \to X$ processes are several orders of magnitude larger than the cross sections for the $A \to X$ process because of their rather large ΔE. For these two processes one can also see the high-energy resonance structures. These are consequences of the avoided crossings with higher $^2\Sigma_g^+$ electronic states, which result in local potential energy minima in the short-range region (for R between 1 a_0 and 2.5 a_0) (Metropoulos et al. 1987). The corresponding potential energy wells then support many shape resonances in the high-energy region (between 1.7 eV and 6.2 eV and between 6.5 eV and 7.9 eV for the $C \to X$ and $E \to X$ processes, respectively). The low-energy resonance structure in the radiative-association cross sections, which is created by the quasi-bound states trapped behind the centrifugal barrier, is the richest for the $C \to X$ process. Only quasi-bound states, which have a symmetry-allowed (i.e. for which the corresponding Hönl-London coefficient is non-zero) bound-state partner supported by the $X^2\Sigma_u^+$ electronic state, contribute to rate coefficients. The resonance structures relevant for the studied

Table 2. Resonance situation overview for the three studied processes of the He_2^+ radiative association.

Process	n_{tot}	n_r	n_w	n_n
$A \rightarrow X$	1	1	1	0
$C \rightarrow X$	480	135	88	47
$E \rightarrow X$	123	68	53	15

Notes. Using formalism of Augustovičová et al. (2012): n_{tot} is the total number of orbital resonances supported by the initial electronic states, n_r is the number of symmetry-allowed resonances, n_w is the number of wide resonances, and n_n is the number of narrow resonances.

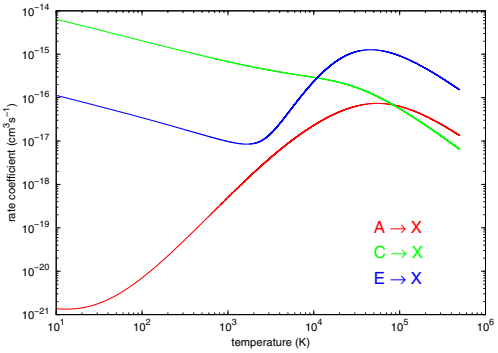

Fig. 2. Rate coefficients for spontaneous (T_b = 0 K) radiative association of He_2^+.

processes are summarized in Table 2. The corresponding rate coefficients for the spontaneous radiative association are shown graphically in Fig. 2, and their values, evaluated at selected temperatures, are provided in Table 3. Our results for the $A \rightarrow X$ process are in excellent agreement with the results of Stancil et al. (1993), indicating thus that in this case the rate coefficients are not very sensitive to the potentials used. For temperatures up to about 10 000 K, the processes $C \rightarrow X$ and $E \rightarrow X$ are dominant, exceeding the $A \rightarrow X$ rate coefficient by several orders of magnitude and thus mimicking the cross-section behaviour.

Cross sections and rate coefficients for the stimulated radiative-association $A \rightarrow X$ process are shown graphically for different black-body radiation temperatures T_b in Figs. 3 and 4, respectively. The difference in cross sections between the limit (T_b = 0 K and T_b = 10 000 K) cases starts to be washed out at collision energies around E = 1 eV. However, at lower energies the difference is almost two orders of magnitude in favour of the stimulated process. The difference in the corresponding rate coefficients at low temperatures (around T = 10 K) reaches two orders of magnitude, although it decreases rapidly with increasing temperature until it becomes negligible at temperatures around T = 10 000 K. The cross sections and rate coefficients for the stimulated $C \rightarrow X$ and $E \rightarrow X$ processes do not vary significantly with the black-body radiation temperatures. This is caused by very large ΔE for these processes, which negates the effect of the black-body radiation temperature in Eq. (6). Consequently one would need the black-body radiation temperature around T_b = 50 000 K to see an increase by merely 1% in the cross sections or rate coefficients.

4. Conclusion

Radiative association formation of the ground $X^2\Sigma_u^+$ electronic state of He_2^+ by spontaneous or stimulated photon emission was investigated considering the lowest three excited $^2\Sigma_g^+$ electronic states ($A^2\Sigma_g^+$, $C^2\Sigma_g^+$, $E^2\Sigma_g^+$) as initial reactant channels. The cross sections for spontaneous radiative association via the $A \rightarrow X$, $C \rightarrow X$, and $E \rightarrow X$ processes were calculated as functions of the collision energy. The corresponding rate coefficients for the formation of He_2^+ in the ground $X^2\Sigma_u^+$ electronic state were determined as functions over a wide range of temperatures. For the $A \rightarrow X$ process, the results were found to be in excellent agreement with those of Stancil et al. (1993). Whereas at low temperatures the $C \rightarrow X$ process is by far the most efficient one (its rate coefficient is more than six orders of magnitude larger than for $A \rightarrow X$), the $E \rightarrow X$ process becomes more efficient at very high temperatures (in the range of 10^4 to 10^5 K) with rate coefficients more than an order of magnitude larger than for $A \rightarrow X$. Stimulation of the radiative association by black-body

Table 3. Values of the total rate coefficients for the three spontaneous processes of the He_2^+ radiative association.

T (K)	$A \rightarrow X$ (cm^3 s^{-1})	$A \rightarrow X$ (1) (cm^3 s^{-1})	$C \rightarrow X$ (cm^3 s^{-1})	$E \rightarrow X$ (cm^3 s^{-1})
10	1.37×10^{-21}	(...)	6.33×10^{-15}	1.13×10^{-16}
20	1.43×10^{-21}	1.44×10^{-21}	4.56×10^{-15}	7.96×10^{-17}
30	1.76×10^{-21}	1.83×10^{-21}	3.73×10^{-15}	6.47×10^{-17}
50	2.78×10^{-21}	2.91×10^{-21}	2.89×10^{-15}	4.97×10^{-17}
100	7.02×10^{-21}	7.18×10^{-21}	2.04×10^{-15}	3.44×10^{-17}
200	2.27×10^{-20}	2.36×10^{-20}	1.45×10^{-15}	2.36×10^{-17}
500	1.30×10^{-19}	1.48×10^{-19}	9.29×10^{-16}	1.41×10^{-17}
1000	5.02×10^{-19}	5.82×10^{-19}	6.75×10^{-16}	9.77×10^{-18}
2000	1.87×10^{-18}	2.16×10^{-18}	5.04×10^{-16}	8.78×10^{-18}
2500	2.79×10^{-18}	3.22×10^{-18}	4.62×10^{-16}	1.04×10^{-17}
3000	3.84×10^{-18}	4.42×10^{-18}	4.32×10^{-16}	1.35×10^{-17}
4000	6.21×10^{-18}	7.13×10^{-18}	3.91×10^{-16}	2.50×10^{-17}
6000	1.16×10^{-17}	1.33×10^{-17}	3.44×10^{-16}	7.02×10^{-17}
8000	1.73×10^{-17}	1.98×10^{-17}	3.15×10^{-16}	1.43×10^{-16}
10 000	2.30×10^{-17}	2.62×10^{-17}	2.93×10^{-16}	2.36×10^{-16}
16 000	3.87×10^{-17}	4.39×10^{-17}	2.48×10^{-16}	5.66×10^{-16}
20 000	4.73×10^{-17}	5.36×10^{-17}	2.24×10^{-16}	7.73×10^{-16}
25 000	5.59×10^{-17}	6.34×10^{-17}	1.98×10^{-16}	9.80×10^{-16}
32 000	6.45×10^{-17}	7.30×10^{-17}	1.69×10^{-16}	1.16×10^{-15}
50 000	7.33×10^{-17}	8.29×10^{-17}	1.16×10^{-16}	1.26×10^{-15}
64 000	7.29×10^{-17}	8.23×10^{-17}	9.13×10^{-17}	1.19×10^{-15}
100 000	6.29×10^{-17}	7.11×10^{-17}	5.56×10^{-17}	9.18×10^{-16}
200 000	3.75×10^{-17}	4.24×10^{-17}	2.31×10^{-17}	4.73×10^{-16}
50 0000	1.34×10^{-17}	1.51×10^{-17}	6.47×10^{-18}	1.51×10^{-16}

Notes. T_b = 0 K.

References. (1) Stancil et al. (1993).

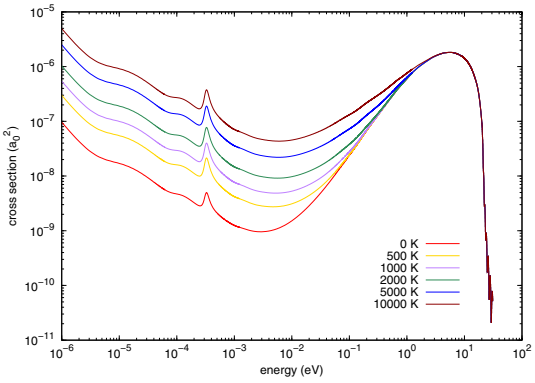

Fig. 3. Cross sections for the stimulated radiative association $A \rightarrow X$ process in He_2^+ for different background temperatures.

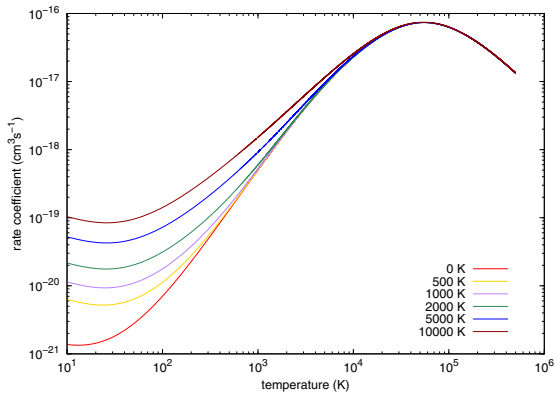

Fig. 4. Rate coefficients for the stimulated radiative association $A \rightarrow X$ process in He_2^+ for different background temperatures.

radiation was shown here to be important for the $A \rightarrow X$ reaction at temperatures up to about 1000 K. For background radiation temperatures of a few thousand K, the increase of the rate coefficient in this temperature range can be by about an order of magnitude and more.

Acknowledgements. L.A. acknowledges funding from the Grant Agency of the Charles University in Prague – GAUK (Grant no. 550112). L.A. and V.Š. also appreciate support of the Czech Science Foundation – GAČR (Grant No. P208/11/0436).

References

Ackermann, J., & Hogreve, H. 1991, Chem. Phys., 157, 75
Augustovičová, L., Špirko, V., Kraemer, W. P., & Soldán, P. 2012, Chem. Phys. Lett., 531, 59
Bawagan, A. D. O., & Davidson, E. R. 1997, Chem. Phys. Lett., 266, 499
Black, J. 1978, ApJ, 222, 125
Carrington, A., Pyne, C. H., & Knowles, P. J. 1995, J. Chem. Phys., 102, 5979
Cencek, W., & Rychlewski, J. 1995, J. Chem. Phys., 102, 2533
Connor, J. N. L., & Smith, A. D. 1981, Mol. Phys., 43, 397
Cooley, J. W. 1961, Math. Comput., 15, 363
Flower, D., & Roueff, E. 1979, A&A, 72, 361
Fontaine, G., Brassard, P., & Bergeron, P. 2001, PASP, 113, 409
Gaur, V. P., Tripathi, B. M., Joshi, G. C., & Pande, M. C. 1988, Ap&SS, 147, 107
Gaur, V. P., Joshi, G. C., & Pande, M. C. 1992, Ap&SS, 197, 57
Harris, G., Lynas-Gray, A., Miller, S., & Tennyson, J. 2004, ApJ, 617, L143
Ho, T. S., & Rabitz, H. 1996, J. Chem. Phys., 104, 2584
Ho, T. S., & Rabitz, H. 2000, J. Chem. Phys., 113, 3960
Huang, Y., & Le Roy, R. J. 2003, J. Chem. Phys., 119, 7398, erratum 2007, J. Chem. Phys., 126, 9904
Ignjatovic, L. M., Mihajlov, A. A., Sakan, N. M., Dimitrijevic, M. S., & Metropoulos, A. 2009, MNRAS, 396, 2201
Koester, D., & Chanmugam, G. 1990, Rep. Prog. Phys., 837, 53
Le Roy, R. J. 2005, LEVEL 7.7: A Computer Program for Solving the Radial Schrödinger Equation CPRR-661
Le Roy, R. J., & Liu, W. 1978, J. Chem. Phys., 69, 3622
Metropoulos, A., Nicolaides, C. A., & Buenker, R. J. 1987, Chem. Phys., 114, 1
Numerov, B. 1933, Math. Comput., 2, 188
Pachucki, K., & Sapirstein, J. 2000, Phys. Rev. A, 63, 504
Ralchenko, Y., Kramida, A. E., Reader, J., & Team, N. A. 2010, NIST Atomic Spectra Database (version 3.1.5), see http://physics.nist.gov/asd3
Soldán, P., & Hutson, J. M. 2000, J. Chem. Phys., 112, 4415
Stancil, P. C. 1994, J. Quant. Spec. Radiat. Transf., 51, 655
Stancil, P. C., & Dalgarno, A. 1997, ApJ, 479, 543
Stancil, P. C., Babb, J. F., & Dalgarno, A. 1993, ApJ, 414, 672
Tung, W., Pavanello, M., & Adamowicz, L. 2012, J. Chem. Phys., 136, 104309
Werner, H.-J., Knowles, P. J., Manby, R. R., et al. 2010, MOLPRO, version 2010.2. A package of ab initio programs, see http://www.molpro.net
Xie, J., Poirier, B., & Gellene, G. 2005, J. Chem. Phys., 122, 310
Yan, Z., & Babb, J. F. 1998, Phys. Rev. A, 58, 1247
Zygelman, B., & Dalgarno, A. 1990, ApJ, 365, 239
Zygelman, B., Stancil, P. C., & Dalgarno, A. 1998, ApJ, 508, 151